THE ASTROPHYSICAL JOURNAL, 327:615–626, 1988 April 15

ISOTHERMALITY OF THE GAS IN THE COMA CLUSTER

JOHN P. HUGHES
Harvard-Smithsonian Center for Astrophysics
KOUJUN YAMASHITA, YOSHIHARU OKUMURA, AND HIROSHI TSUNEMI
Department of Physics, Faculty of Science, Osaka University
AND
MASARU MATSUOKA
Institute of Space and Astronautical Science, Tokyo
Received 1987 April 9; accepted 1987 October 1

ABSTRACT

We analyze the spectral and spatial X-ray data for the Coma cluster using nonisothermal temperature distributions. The spectrum was obtained by the Japanese X-ray satellite *Tenma* and the spatial data came from a reanalysis of the *Einstein Observatory* images. The superior energy response of the *Tenma* instrument allows us to determine the iron abundance more accurately than before; a value of between 16% and 32% (independent of model), relative to the cosmic value, is indicated. We find that the X-ray data alone can be described adequately by either an isothermal or an adiabatic gas temperature distribution. However, the cluster gravitational potentials inferred for the two models are quite different. If the temperature distribution is isothermal (or nearly so), then the cluster binding mass increases as r^1 for large radii, and we derive a binding mass of $\sim 1.5 \times 10^{15}\ M_\odot$ within 3 Mpc ($H = 50$ km s^{-1} Mpc^{-1}). If the gas temperature is adiabatic, then the binding mass must be considerably more centrally condensed than the galaxies or the gas; over 90% of the cluster mass is contained within 1 Mpc. Nevertheless, this solution is not self-consistent since the total binding mass density drops below the inferred gas density at ~ 1 Mpc. Neither of these models is entirely satisfactory from our point of view, and so, based on theoretical considerations of thermal conduction in the intracluster medium, we propose a hybrid model consisting of a central isothermal region surrounded by a polytropic distribution. We determine limits on the size of the isothermal region as a function of the central, isothermal temperature, and we find that as much as 75% of the global emission can be coming from the isothermal component.

Subject headings: galaxies: clustering — galaxies: intergalactic medium — galaxies: X-rays

I. INTRODUCTION

Since the discovery of hot gas within clusters of galaxies, researchers have eagerly sought to determine the temperature and density structure of the plasma. With this information, and the single assumption of hydrostatic equilibrium, one can in principle determine the total binding mass of the cluster, allowing a direct determination of the ratio of luminous to nonluminous matter (see, e.g., Sarazin 1986). Whether or not the gas in clusters of galaxies is truly isothermal also has important implications. Recently, various authors (Bertschinger and Meiksin 1986; Friaca 1986; Rosner, Tucker, and Najita 1988) have studied the effects of thermal conduction on the formation and evolution of cooling flows. Conduction tends to have dramatic effects, in some cases reducing the derived mass flow rates by as much as one order of magnitude. If it can be shown that clusters without cooling flows (such as Coma) contain significant isothermal regions, this might indicate that conduction is a widespread phenomenon in clusters.

At the present time for most clusters, though, this program is hampered by several factors, such as the need to parameterize the radial dependencies involved, the lack of imaging data at large core radii and the problem of determining the temperature structure from global integrated cluster X-ray spectra. Nevertheless as instrumentation improves, some of these problems will be mitigated, and we can expect improvements in our understanding. In this paper we report on our investigation of the density and temperature structure of the gas in the Coma cluster using data obtained by the broad-band X-ray spectrometer onboard the Japanese X-ray satellite *Tenma*. This instrument consists of an array of gas scintillation proportional counters (GSPCs) which offer improved spectral resolution over ordinary proportional counters in the energy range above ~ 1 keV. These data allow us to make considerably more precise measurements than before of the Kα iron line emission, as well as the overall X-ray continuum. We also present results from a reanalysis of the imaging proportional counter (IPC) data from the *Einstein Observatory*, in which we utilize an additional off-center pointing of Coma to define the X-ray surface brightness profile out to $\sim 40'$. This is nearly twice the radial extent used in previous studies, and as we show in § III, enables us to set stringent limits on the acceptable nonisothermal models.

The Coma cluster is nearby ($z = 0.0235$; Sarazin, Rood, and Struble 1982), and both extended and luminous in X-rays, making it an excellent testbed for studies of the hot intracluster gas. Various studies of its X-ray surface brightness, using data obtained by the IPC (Abramopoulos, Chanan, and Ku 1981) as well as earlier rocket data (Gorenstein *et al.* 1979), have resulted in a fairly well-defined profile for the gas density, but only within about the inner two core radii. However, the *Einstein Observatory* made a series of pointings near the center of Coma, and we have merged the data from them. Later in this

paper we present results of fits of nonisothermal models to the X-ray surface brightness data.

The integrated X-ray spectrum of Coma also has been well-determined over the past 10 yr, a result of observations using *Uhuru* (Kellogg, Baldwin, and Koch 1975), *Ariel 5* (Mitchell *et al.* 1976), *OSO 8* (Serlemitsos *et al.* 1977; Mushotzky *et al.* 1978), and *HEAO* 1 A-2 (Henriksen and Mushotzky 1985, 1986). All but the most recent data were adequately described by an isothermal temperature distribution of $\sim$7–8 keV. However, an analysis of the *HEAO* 1 A-2 data for Coma has led the latter two authors to the conclusion that the cluster temperature distribution is far from isothermal, based on a new model-independent approach which they have developed. We have found that this approach is internally inconsistent over a large range of parameter space (see also Cowie, Henriksen, and Mushotzky 1987).

As a convenient parameterization for nonisothermal temperature distributions we first considered the polytropic models developed by Cavaliere and Fusco-Femiano (1976, 1978). In these models, the distributions of the galaxies and the X-ray emitting gas are related through their common gravitational potential. The galaxies are assumed to be isothermal, and the gas temperature distribution follows the gas density distribution as $T \propto \rho^{\gamma-1}$, where γ, the polytropic index, is taken to be a constant. Conditions of isothermality and adiabaticity within the cluster gas are represented by values for γ of 1 and 5/3, respectively. We will show in this paper that fits to the imaging and spectral X-ray data for this model imply that the cluster temperature distribution is nearly isothermal, while an adiabatic temperature distribution can be rejected with high confidence.

Such intermediate values of the polytropic index are believed to represent more "complicated" physical situations which might include thermal conduction, radiative cooling, local heating, evolutionary effects, etc. However, it has been consistently stressed (Perrenod 1978; Friaca 1986) that realistic models which consider the evolution of the cluster gas within a physical framework do not resemble polytropes. In light of this and as a first attempt to explore possible temperature distributions which are not purely polytropic, we have constructed a hybrid model consisting of an isothermal core surrounded by a polytropic region. This can be considered to be a two-component polytropic model, in which we fix the indices and instead vary the radius at which the distribution changes. This model is strongly motivated by the fits to the imaging data, which are tightly constrained to be near-isothermal within the center. The polytropic region outside then gives rise to the nonisothermal component which appears in the global spectrum. We find that the spectral data can be fitted with an isothermal region contributing from $\sim$20% to as much as 75% of the total observed emission. This model is entirely consistent with both the imaging and spectral X-ray data.

The article is organized as follows. In § II we discuss some features of polytropic models in general as well as the particular formulations of Cavaliere and Fusco-Femiano (1976, 1978) and Henriksen and Mushotzky (1985, 1986). The IPC imaging data and corresponding model fits are in § III. Section IV contains a discussion of the spectral observations obtained by *Tenma*. Fits of polytropic models to these data are also presented here. Discussion of the cluster binding masses implied by the several models appear in § V. Later in this section, the hybrid model is developed and fitted to the spectral data. Final remarks are in § VI.

II. POLYTROPIC MODELS

The distribution of the hot plasma in clusters of galaxies is determined in large part by the gravitational potential of the cluster. Since the cluster galaxies respond to the same potential, it is possible to relate their space distribution to that of the gas. This is accomplished through the relationship

$$\frac{1}{\rho}\frac{dp}{dr} = \frac{1}{\rho_G}\frac{dp_G}{dr}. \tag{1}$$

The actual distribution of either the galaxies or the gas depends on assumptions about the galaxy velocities or the gas temperature. Cavaliere and Fusco-Femiano (1976, 1978) have shown that when the galaxy velocities are assumed to be isothermal and the gas temperature is polytropic ($p \propto \rho^{\gamma}$), it is possible to determine the radial run of both the gas density and temperature of the cluster. For $\gamma \neq 1$ they find

$$\frac{T}{T_0} = \left(\frac{\rho}{\rho_0}\right)^{\gamma-1} = 1 - \frac{3}{2}\frac{\gamma-1}{\gamma}\beta \ln(1+y^2), \tag{2}$$

and for $\gamma = 1$,

$$\frac{\rho}{\rho_0} = (1+y^2)^{-3\beta/2}, \tag{3}$$

where we have used the convenient approximation, $\rho_G = \rho_{G0}(1+y^2)^{-3/2}$ (King 1972) for the galaxy space distribution and set $y \equiv r/r_c$. This approximation to an isothermal sphere is entirely adequate for our purposes since the imaging X-ray data extend only to $\sim$40′ ($\sim$5 core radii), and the bulk of the observed *Tenma* emission comes from within this region as well. The parameter β is the ratio of gas to galaxy temperature, expressed as $\beta \equiv \mu m_H v_{\rm los}{}^2/kT$, where $v_{\rm los}$ is the galaxy line-of-sight velocity dispersion (Bahcall and Sarazin 1978) and T is either the isothermal temperature or the central temperature for the polytropic models.

In this model there are five relevant parameters which are to be determined by fits to the X-ray data: T_0, the central gas temperature; ρ_0, the central gas density; r_c, the core radius; γ, the polytropic index; and β, the ratio of galaxy to gas effective temperature, which also can be considered to represent the slope of the gas density versus radius relation (as in eq. [3]). In practice it is possible to carry out the imaging and spatial analysis separately; this is a result of the limited high-energy response of the *Einstein* mirrors and the large field of view of the *Tenma* instrument. The imaging data put constraints on the allowed values for r_c, β, and γ; while the spectral data constrain T_0 and γ. Normalizations to both the imaging and spectral data determine ρ_0.

We have been unable to obtain acceptable fits to the X-ray imaging data for any value of β or r_c for an adiabatic model ($\gamma = 5/3$) with the form given by equation (2). This is also the case for other versions of the polytropic model. For example, we have fitted the imaging data using the alternate form of the polytropic model given by Lea (1975) and found that again no adiabatic model was allowed. Recall that both of these models assume that the cluster gravitational potential is traced by the galaxies. In order to obtain an acceptable fit for an adiabatic temperature distribution, we have had to relax this assumption. The polytropic model which we derive immediately below is consistent with the Bahcall and Sarazin (1978) general polytropic model for an arbitrary cluster potential.

In order to vary the shape of the cluster potential, we employ a simple generalization of equation (2), in which we introduce a

single additional parameter, of the form

$$\frac{T}{T_0} = \left(\frac{\rho}{\rho_0}\right)^{\gamma-1} = 1 - \frac{3}{2}\frac{\gamma-1}{\gamma}\frac{\beta}{\alpha}[1-(1+y^2)^{-\alpha}] . \quad (4)$$

This reduces to equation (2) when $\alpha = 0$. The limit $\alpha \leq \frac{1}{2}$ must be imposed to avoid having the virial density drop below zero at a finite radius. We show below (§ III) that an isothermal gas temperature distribution requires values of α near 0, while an adiabatic distribution requires values near $\frac{1}{2}$. Note that this equation is not a solution of the hydrostatic equilibrium equation (eq. [1]) for an isothermal galaxy velocity distribution. Instead our purpose here is to introduce a convenient parameterization for the cluster potential and then determine limits on those parameters under the assumption that the gas temperature distribution is adiabatic.

Based on simple assumptions, viz., hydrostatic equilibrium and the ideal gas law, one can derive an expression for the cluster binding mass which depends only on the gas density and temperature. For polytropic models, the relationship can be further reduced and written in terms of the density (or temperature) only and is given by

$$M(<r) = -\frac{kT_0}{\mu m_H G n_0}\gamma r^2\left[\frac{n(r)}{n_0}\right]^{\gamma-2}\frac{dn(r)}{dr} . \quad (5)$$

For the density distribution given by equation (4):

$$M(<r) = 5.4\times 10^{14}\left(\frac{r_c}{0.5\ \mathrm{Mpc}}\right)\left(\frac{T_0}{10\ \mathrm{keV}}\right)\beta\frac{y^3}{(1+y^2)^{\alpha+1}}\,M_\odot , \quad (6)$$

where $\mu = 0.61$, appropriate to a fully ionized plasma with 10% helium by number. At large core radii the cluster binding mass increases with radius as $r^{1-2\alpha}$. We can see that including the additional parameter α allows us to vary the shape of the cluster binding mass distribution as well as its radial scale.

Henriksen and Mushotzky (1985, 1986) have recently tried to extend the analysis of cluster X-ray spectra to include non-isothermal temperature distributions in a model-independent way. Their approach was to use equation (3) (the isothermal gas relationship) to describe the form of the radial density variation for the gas, which then was coupled with the polytropic relationship to determine the temperature distribution. Although in this approach the gas temperature and density distributions lack any clear physical connection with the galaxy distribution, it nevertheless is a useful parameterization of the possible temperature variation and we do employ it in our so-called hybrid model. However, hydrostatic equilibrium is not guaranteed for arbitrary choice of γ and β in this model. To demonstrate this, consider the mass distribution, which is given by

$$M(<r) = 5.4\times 10^{14}\left(\frac{r_c}{0.5\ \mathrm{Mpc}}\right)\left(\frac{T_0}{10\ \mathrm{keV}}\right)\times\beta\gamma\frac{y^3}{(1+y^2)^{3\beta(\gamma-1)/2+1}}\,M_\odot , \quad (7)$$

The limiting form of equation (7) for large core radii is $y^{1-3\beta(\gamma-1)}$, which is zero if $\beta(\gamma-1) > \frac{1}{3}$. In that case, the binding mass distribution reaches a maximum at $y_m = [\beta(\gamma-1)-\frac{1}{3}]^{-1/2}$ and then falls to zero at infinity. In order to avoid negative mass or, equivalently, to avoid a cluster gravitational potential which falls off faster than a point mass potential, this approach requires that the cluster be nonhydrostatic. Physically, a parcel of gas at large radius has a temperature which is too low for it to be stable against infall, given a realistic cluster potential. An artificial cutoff in the parameters,

$$\gamma < 1 + \frac{1}{3\beta} \quad (8)$$

(see Cowie, Henriksen, and Mushotzky 1987) must be imposed for consistency since y_m can be as small as 2, well within the region from which we actually see gas at X-ray temperatures.[1]

III. SPATIAL ANALYSIS

The most extensive X-ray imaging data for the Coma cluster were those taken by the IPC on the *Einstein Observatory* (see Giacconi *et al.* 1979 for a description of the instrumentation). There were three pointings made: one approximately at the cluster's center and two offset from this north and south by $\sim 20'$. Since the active region within the IPC rib support structure is $\sim 40'$ wide, previous studies which utilized only the central field were confined to a maximum radial coverage of only $\sim 20'$. With the additional fields, it is possible to double this coverage. As we show below, this additional radial coverage allows us to discriminate against a large class of models.

a) Data

In order to combine the surface brightness data from the various fields it was necessary to compensate for various detector dependent effects. The gain of the detector varied from observation to observation as well as across the focal plane. For two of the fields (I1793, the central region, and I1792, the northern region) the average gains were the same (BAL $\approx$ 15), but the gain for the southern pointing (I1790) was abnormally high (BAL $\approx$ 20), which resulted in a skewed distribution for the pulse height spectrum. We have not pursued the analysis of the southern field. Spatial variations in the counter gain (especially for extended sources) are largely taken care of through the use of data extracted from pulse-height invariant energy bins.

Another effect arises from the geometrical vignetting of the telescope mirrors. This is a function of both the incident photon energy and position in the counter and evidences itself by a decrease in effective area at off-axis locations. We determined the correction to be applied at several radial positions using a hard spectrum ($kT \approx 10$ keV, folded through the mirror and instrument response), appropriate to the Coma cluster. The correction varies from 1 (on-axis) to ~ 1.6 (20′ off-axis). As the raw data were extracted from the images, the count rates were multiplied by a vignetting correction which was the average over the region from whence the counts came.

For both the central and northern fields the data (in the energy range 0.5–4 keV) were taken from annuli of size 1.8 binned about the cluster X-ray center, given by Abramopoulos, Chanan, and Ku (1981) as $\alpha_{1950} = 12^h57^m19^s$, $\delta_{1950} = 28°13'07''$. Background subtraction was performed in detector coordinates using a long exposure pointing toward a source-free region of the sky which had very nearly the same detector gain. In order to avoid the IPC rib support structure, data

[1] For Coma with $\beta = 0.76$, eq. [8] eliminates all polytropic indices greater than 1.43 and in fact forces us to reject *a priori* most of the allowed parameter space derived from the *HEAO* 1 A-2 analysis (see Fig. 7 in Henriksen and Mushotzky 1986). Hence, cluster masses derived from this approach should be viewed with some suspicion.

from only the inner 20′ × 20′ of each field were used. In the case of the central pointing that meant restricting the maximum radial annulus to $R \leq 20'$, since the center of this field was also approximately the center of the cluster. The situation was more complicated for the northern field, since here the cluster center was near the edge of the field. Angular ranges for each annuli were determined, which defined the region within the ribs. Counts were extracted from several (usually three or four) subregions within this angular range, so that an appropriate average vignetting correction could be applied, as discussed above. Excellent agreement was found between the data from the northern field and the data from only the northern sector (−45°, 45°) of the central field, in the radial region of overlap (9′–20′). The northern field also contained two point sources (a Seyfert galaxy and presumably a background quasar) which were detected by the standard IPC processing algorithm; counts from within a 3′ radius centered on each of these were excluded.

The errors on the counts were increased over the purely statistical ones to account for two possible sources of systematic effects. The first was the inclusion of an error equal to 20% of the background rate. This is about the size of the observed variation in background from field to field (Abramopoulos, Chanan, and Ku 1981). Second, because of nonuniformities in the spatial scale of the IPC, we included a 6% systematic error as well (D. Fabricant 1986, private communication). Both additional errors were added in quadrature to the statistical error.

b) Analysis

Surface brightness profiles for nonisothermal cluster models were generated for the parameters α, β, γ, and r_c. To approximate the spatial response of the IPC we convolved the models with a circular Gaussian of width 1.′4 (FWHM). The central temperature for each parameter set was determined by requiring that the average temperature within 3° (the *Tenma* field of view) be 7.5 keV. As we mention below, this is an accurate way to characterize the X-ray spectrum; furthermore, the response of the IPC is virtually flat for temperatures above ∼2 keV, and thus the actual value of the central temperature does not greatly influence our results. We also set the fractional elemental abundances to 25%. The spatial analysis was carried out separately for the northern data (angular range approximately −45° to 45°, radial range 0′ to 40′) and the central data (angular range 0°–360°, radial range 0′–20′). The results from the two regions are quite different for at least two reasons: (1) the ellipticity of the cluster, which is averaged over in the data from the central region, and (2) the larger radial extent of the northern region.

In Figure 1 we plot the X-ray surface brightness of the Coma cluster for the data from the northern region, along with the best-fit isothermal model. Beyond ∼17′, the data are clearly well fitted by a single power law in surface brightness versus radius with slope about −2.7, implying a gas density versus radius slope of ∼0.62 (the parameter β in our model). This is confirmed by our detailed fits to these data using the Cavaliere and Fusco-Femiano (1976, 1978) polytropic formalism with $\alpha = 0$. In Figure 2*a* we present the results of these fits for β and γ, in the form of two-dimensional χ^2 contours (99% confidence level with $\chi^2_{\rm min} + 9.2$; Avni 1976; Lampton, Margon, and Bowyer 1976). Recall that β effectively represents the radial falloff of the density profile (higher β-values correspond to steeper profiles), while γ characterizes the radial temperature dependence (from isothermal, $\gamma = 1$, to adiabatic, $\gamma = 5/3$). The importance of including the imaging data from the northern field can be dramatically demonstrated by comparing the dashed contours (corresponding to the central data set) with the solid contour (the northern data) in Figure 2*a*. The data from the northern region require that we reject all polytropic indices greater than ∼1.2 at the 99% confidence level. No such statement can be made based on the central region alone, where all polytropic indices are accepted. This is a result of the

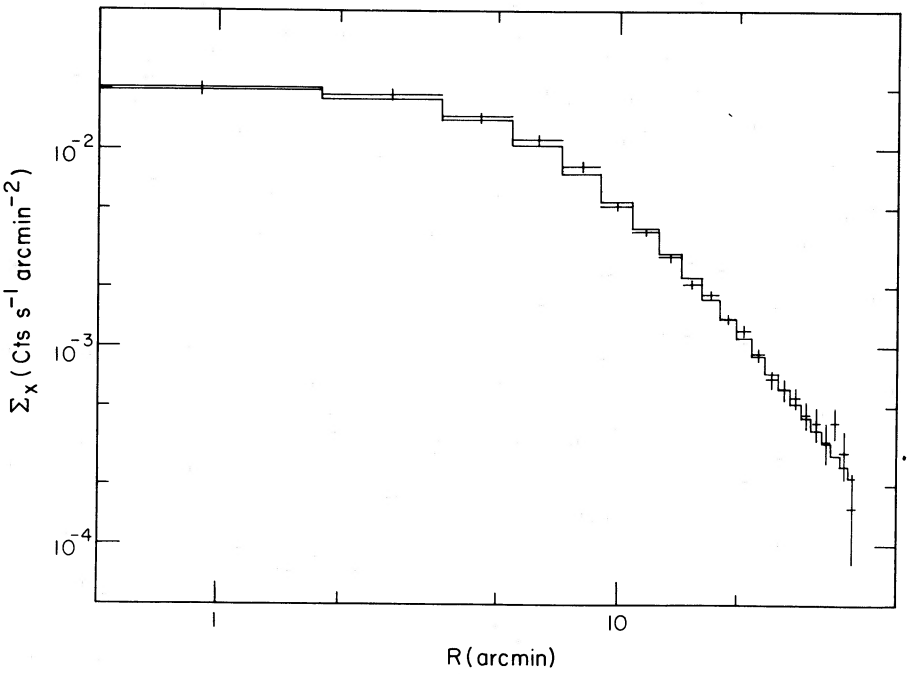

FIG. 1.—Radially averaged IPC X-ray surface brightness of the Coma cluster with best-fit isothermal model

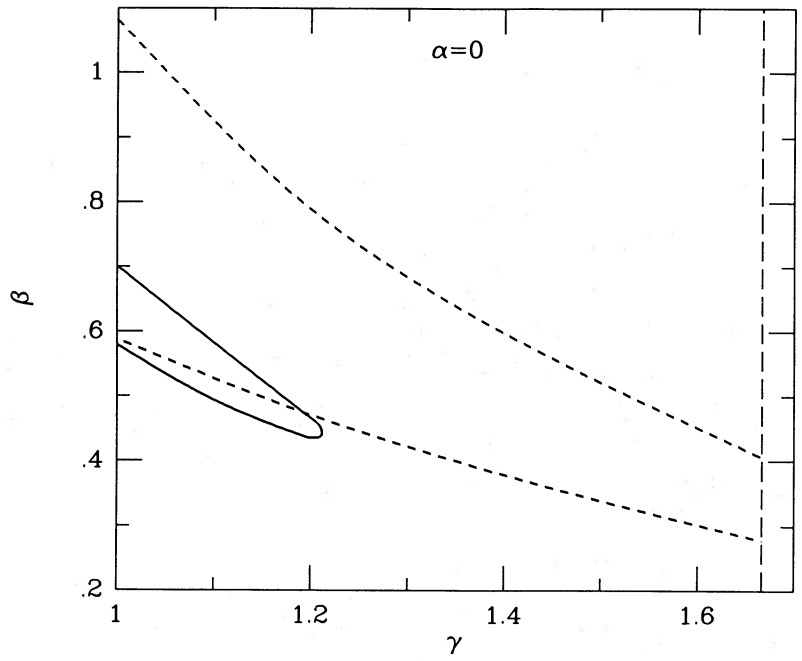

FIG. 2a

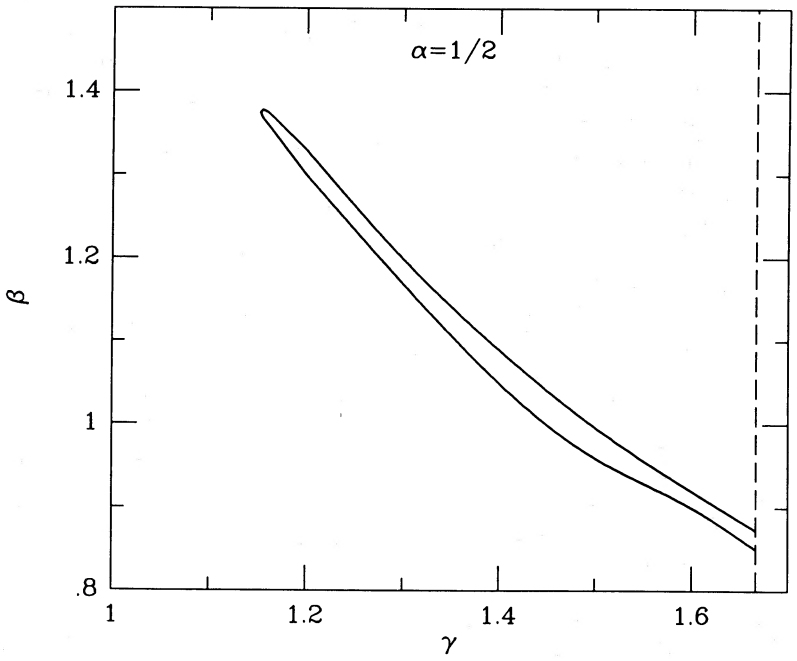

FIG. 2b

FIG. 2.—(*a*) Results of fits to the IPC surface brightness profile using data from the central field only (*dashed lines*) and including data from the north (*solid lines*). Two-dimensional χ^2 contours (99% confidence level) for β versus γ using the Cavaliere and Fusco-Femiano (1976, 1978) model ($\alpha = 0$). The limit $\gamma = 5/3$ corresponding to the adiabatic condition is marked by the vertical dashed line to the right. (*b*) Same as (*a*) but for the $\alpha = \frac{1}{2}$ polytropic model.

limited spatial coverage of this data set. The decrease of β with increasing γ arises naturally in this model, since β is the ratio of the effective galaxy temperature to the *central* gas temperature. Since the temperature doubles from isothermal to adiabatic (see Fig. 5 below), β is approximately halved over the same range. Table 1 presents the results of these fits to the northern data set specifically for the isothermal model for the parameters r_c, β, and n_0 (number density of hydrogen atoms) with 90% errors and gives the χ^2 values. Note that we use a value for the Hubble constant of 50 km s^{-1} Mpc^{-1}. The errors on n_0 were increased to include a factor of 3 variation in hydrogen column density to the source. This additional error was roughly the same size as the error obtained from direct fits to the model. As a check on our data extraction and model fitting techniques, we have compared the fitted parameter values from our central field data alone with the published work of

TABLE 1

BEST-FIT SPATIAL PARAMETER VALUES FOR COMA CLUSTER FROM IPC DATA

Parameter	Isothermal ($\alpha = 0$)	Adiabatic ($\alpha = \frac{1}{2}$)
r_c	7.6 ± 0.7	5.5 ± 0.4
β	0.63 ± 0.03	0.86 ± 0.01
n_0 ($\times 10^{-3}$ cm^{-3})[a]	2.6 ± 0.3	3.1 ± 0.4
χ^2 ($\nu = 18$)	12.8	16.2

[a] $H = 50$ km s^{-1} Mpc^{-1}.

Abramopoulos, Chanan, and Ku (1981). Our values, $\beta = 0.75 \pm 0.12$ and $r_c = 10.8 \pm 2.0$, are in excellent agreement with their isothermal models.

The functional form for the gas density utilized above is rather specific, and thus the preceding result does not imply that all possible adiabatic models are unacceptable. We have found that an acceptable fit to the imaging data for an adiabatic model can be obtained for the generalized model (eq. [4]) with $\alpha = \frac{1}{2}$. In Figure 2*b* we present the results of these fits for β and γ, in the form of two-dimensional χ^2 contours, again at the 99% confidence level, but only for the data from the northern region. Notice that in this case models with $\gamma < 1.15$ can be rejected. The fitted parameter values for the adiabatic model are shown in the final column in Table 1.

We must stress, however, that the constraints on γ derived in this analysis and shown in Figures 2*a* and 2*b* arise almost totally from the form of the radial density variation in the model and not from the temperature distribution. This is because the cluster temperature remains high, i.e., above the IPC bandpass, until the density has fallen to rather low values. Nevertheless in the context of the present model, this distinction is irrelevant and our constraint on the polytropic index determined in this manner from the imaging data is valid. It also is possible, however, to make some statement about the gas temperature distribution by examining the X-ray spectrum of the cluster. This is the subject of the next section, in which we compare various polytropic models with the *Tenma* spectral data.

IV. SPECTRAL ANALYSIS

a) Data

The spectral observations of the Coma cluster described in this paper were carried out by the second Japanese X-ray satellite, *Tenma*. Details of the satellite system are reviewed by Tanaka *et al.* (1984) and the X-ray counters by Koyama *et al.* (1984). Briefly, the instrument consists of a large effective area (640 cm^2) array of GSPCs, whose main advantage is superior spectral resolution, ~9.5% (FWHM) at 5.9 keV, which is approximately half that of ordinary proportional counters. The counters are combined into two groups (SPC A and SPC B) of four units with each group having a slightly different field of view (2°.5 and 3°.1 FWHM, respectively). Overall counter performance (linearity, stability) remained excellent since the launch on 1983 February 20 to the termination of operations in early 1986.

Inflight calibration is performed continuously using a ^{109}Cd source, which emits a line at 22.10 keV due to the Kα transition in silver. Flourescence of thorium (a contaminant of the beryllium window) produces the Lα line at 12.97 keV. Another useful calibration line occurs at 8.04 keV (copper Kα), a result of particle and X-ray interactions in the bronze collimator. Using these lines an energy scale, accurate to 30 eV, has been obtained. For the Coma cluster, this calibration procedure was applied to the data from each of the individual counter units and a common energy scale was established. Furthermore, observations of the cluster were carried out in a low and a high gain mode and then reduced to the same scale.

The Coma cluster was observed early in the mission: 1983 March 25–26 (low gain) and 1983 March 28–31 (high gain). The exposure times were 1.59×10^4 s and 1.69×10^4 s. Background measurements, in a nearby source-free region of the sky, were taken for three days before and one day after the on-source observations. The data were reduced and the background was subtracted as described in Okumura *et al.* (1988). The spectrum is statistically well-determined over the energy range from ~1.5 keV–15 keV, since several times 10^5 source photons were obtained. However, the statistical errors are increased by the introduction of a 1% systematic error as described in Koyama *et al.* (1984), which is necessary to account for nonuniformities in the pulse height channel widths (of this order) due to electronic noise in the analog-to-digital converters.

The initial analysis of the *Tenma* data for the Coma cluster was carried out by Okumura *et al.* (1988). These authors utilized a single temperature thermal bremsstrahlung continuum with a best-fit temperature of 8.2 ± 0.3 keV. The Gaunt factor used was that given by Matteson (1971) with corrections (nonrelativistic) due to electron-electron bremsstrahlung (Maxon and Corman 1967). Iron emission lines, both Kα and Kβ, were included as Gaussian lines with width small compared to the counter energy resolution and with energies and equivalent widths determined by fitting to the data to minimize χ^2. The line centroids were consistent with the cluster's optical redshift ($z = 0.0235$), and in fact the fitted energy of the iron Kα line can be used to determine the cluster redshift independently, $z = 0.028 \pm 0.007$ (90% error). This latter check is possible because of the superior energy resolution of the GSPCs onboard *Tenma* in comparison to the standard proportional counters used in the past. Furthermore, it confirms the accuracy of our energy scale (to better than 1%) and detector response matrix.

We have extended the above analysis to include thermal emission from more realistic plasma models (J. C. Raymond 1986, private communication; Raymond and Smith 1977, hereafter RS). In addition, we have assumed both a purely isothermal temperature distribution as well as the polytropic models discussed above, in each case setting limits on the allowed temperatures and iron abundances required by the observations.

b) Isothermal

We are able to obtain acceptable fits to the Coma data for a single temperature plasma with a single value for the iron abundance. Figure 3 shows the data and best-fit model with $kT = 7.5$ keV and an iron abundance of ~21% of the cosmic value (assumed to be 4.0×10^{-5} throughout this analysis). Table 2 shows the best-fit values and 90% errors for the temperature, elemental abundance (as a fraction of cosmic, see below), and emission measure ($n_0^2 r_c^3$), in addition to the χ^2 value. Because of the thickness of the beryllium window (~100 μm) on the GSPCs, we are unable to constrain values of source column densities lower than $\sim 10^{22}$ H atoms cm^{-2} for any of the models presented here. The central gas density from the normalization to the *Tenma* spectrum is $(2.6 \pm 0.1) \times 10^{-3}$ cm^{-3} using the fitted core radii from Table 1. This value is in

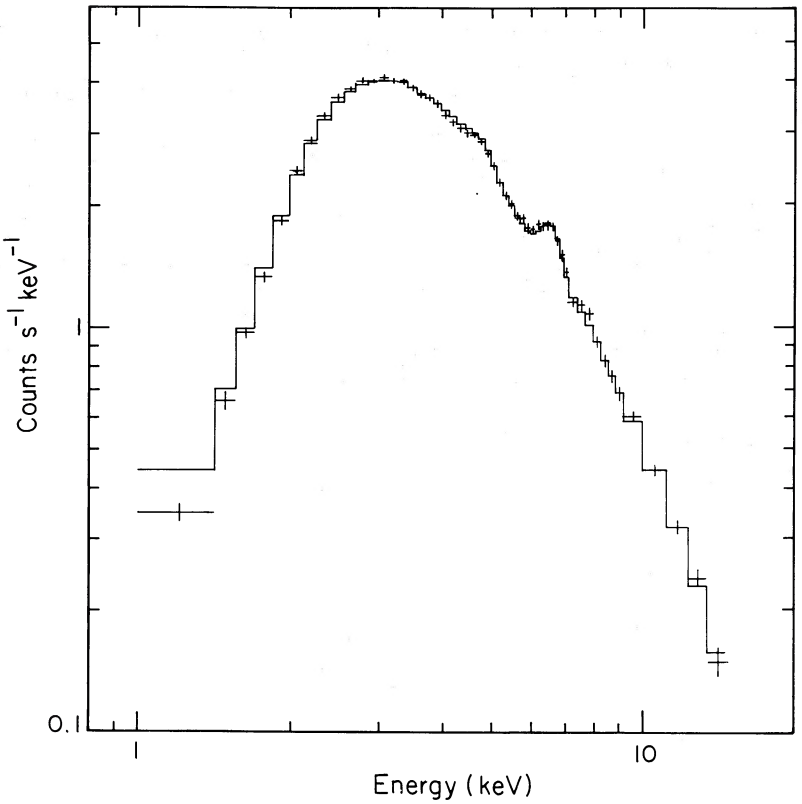

FIG. 3.—*Tenma* X-ray spectrum of the Coma cluster with best-fit isothermal model

excellent agreement with the central density determined from the normalization to the IPC surface brightness. In our fitting procedure we explicitly include the cluster's redshift, using the optically determined value given above. As can be seen in Figure 3, there are no systematic deviations between the data and best-fit isothermal model, particularly at high and low energies.

To determine the elemental abundance in the cluster, our approach throughout this work was to fix the relative abundances of the elements with $Z \geq 12$ at their cosmic values and then vary the overall fractional abundance. These are the elements with K-shell emission lines falling within the *Tenma* bandpass. It should be noted that the decrement value is virtually the same whether or not the abundance of elements other than iron are varied. Okumura *et al.* (1988) have derived a slightly larger value for the iron abundance of Coma using the same data. Part of this difference (about half) arises from the different analysis procedures; their method involves fitting the iron line with a Gaussian line profile of variable intensity and line width. From this and the continuum intensity they determine an equivalent width, which is larger than ours because of the finite width of the fitted line. They then derive the iron abundance by comparing to an independent calculation for the thermal emission from an optically thin plasma in collisional equilibrium (K. Masai 1984, private communication), which accounts for the remainder of the discrepancy. Differences of 30% or so between such models are not unexpected due to uncertainties in the atomic physics (J. C. Raymond 1986, private communication).

TABLE 2

BEST-FIT SPECTRAL PARAMETER VALUES FOR COMA CLUSTER FROM *TENMA* DATA

Parameter	Isothermal ($\alpha = 0$)	Adiabatic ($\alpha = \frac{1}{2}$)
T (keV)	7.5 ± 0.2	20.5 ± 0.8
Abundance[a]	0.21 ± 0.03	0.27 ± 0.03
$n_0^2 r_c^3$ (10^{66} cm^{-3})[b]	5.9 ± 1.2	4.3 ± 0.6
χ^2 ($\nu = 56$)	72.8	75.2

[a] Fraction of cosmic value (4.0×10^{-5} iron atoms per hydrogen).

[b] $H = 50$ km s^{-1} Mpc^{-1}.

The difference in derived temperature between the simple bremsstrahlung emission model employed by Okumura *et al.* (1988) and that of the RS emission model used here can be explained as a result of the inclusion of additional emission processes (such as free-bound and two-photon continuum) in the RS model. In particular, recombination radiation, i.e., free-bound, contributes to the emission above the Fe-edge, leading to the slightly lower temperature value obtained here. Because of these additional processes the RS emission model is expected to be more realistic in this situation.

We have also determined the joint error region for temperature versus iron abundance. In Figure 4*a* we show the error contours at the 90% and 99% confidence level ($\chi^2_{\rm min} + 4.6$ and $\chi^2_{\rm min} + 9.2$; Avni 1976; Lampton, Margon, and Bowyer 1976) for the joint estimation of two parameters. The iron line at these temperatures is a blend of Kα emission from He-like and H-like ions and, although the *Tenma* GSPCs cannot resolve these separate lines, their relative intensities do influence the expected line shape as well as the energy centroid.

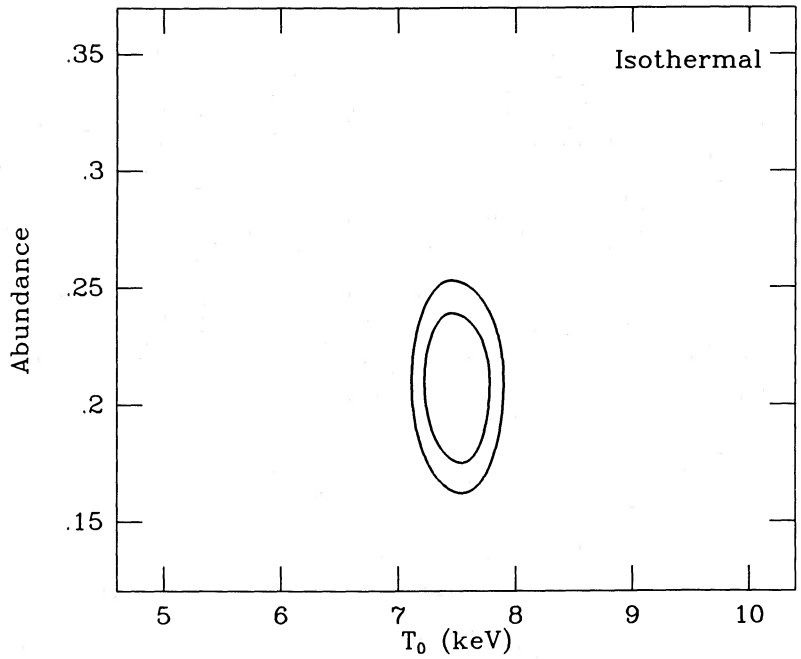

FIG. 4*a*

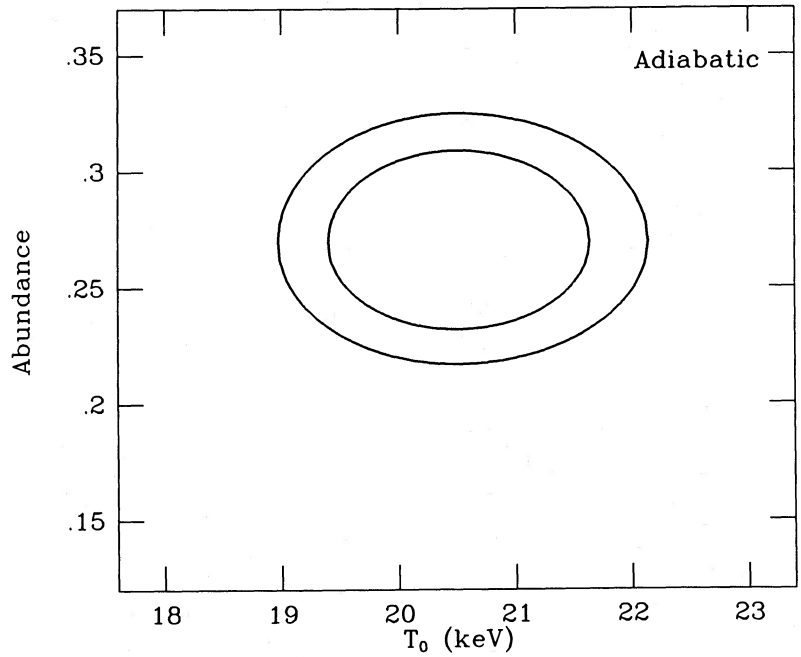

FIG. 4*b*

FIG. 4.—(*a*) Results of fits to the *Tenma* X-ray spectrum of Coma. Two-dimensional χ^2 contours (90% and 99% confidence levels) for fractional iron abundance versus temperature using the isothermal model. The cosmic iron abundance is assumed to be 4.0×10^{-5} relative to hydrogen. (*b*) Same as (*a*) but for the adiabatic model. Uses the modified Cavaliere and Fusco-Femiano (1976, 1978) model with $\alpha = \frac{1}{2}$. Central temperature is denoted by T_0.

c) Comparison to the HEAO 1 A-2 Coma X-Ray Spectrum

Our fitted values of temperature and iron abundance for the isothermal model are in moderate agreement with those of the *HEAO* 1 A-2 X-ray spectrum of Coma (Henriksen and Mushotzky 1986). However, we feel that these authors have overstated the significance of their results, specifically with regard to the limits on the polytropic index, which is constrained to lie between 1.4 and 1.6 in their work. Our main criticism is that they do not include any nonstatistical error (e.g., systematic error) in their analysis (R. F. Mushotzky 1986, private communication). Systematic uncertainties in the pulse height–energy calibration of their instrument of at least 1% (either through temporal gain changes or uncertainties in the fitted energies of calibration lines) should be included. In addition, the check on the energy calibration arising from fitting the

cluster's redshift, which was carried out for the *Tenma* GSPC data, is not possible for the *HEAO* 1 A-2 data because of the poorer spectral resolution of these detectors. We emphasize that the determination of a nonisothermal temperature distribution is a higher order fit to the data than just the determination of the average temperature and as such requires much more careful attention to possible instrumental uncertainties and systematic errors. In fact with data of high statistical accuracy the challenge is to obtain acceptable fits for an isothermal model (given a true isothermal source distribution). Any systematic effects tend to favor nonisothermal models, simply because the parameter space available to these models is so much larger. Only when possible systematic effects in the data have been identified or removed can an isothermal model be rejected with confidence.

d) Standard Cavaliere and Fusco-Femiano Polytropic Models ($\alpha = 0$)

In order to determine the extent of isothermality implied by the *Tenma* data and to follow up the imaging analysis of § III, we have carried out fits to the X-ray spectrum using the standard Cavaliere and Fusco-Femiano polytropic temperature distribution (eq. [2]). The spectral data are most sensitive to the parameters T_0, the central gas temperature, and γ, the polytropic index, but also have some dependence on β. Specifically, the fitted central temperature tends to increase with decreasing β. For the adiabatic case, a decrease in β of ~ 0.1, results in an increase in central temperature of 1–2 keV. However, since there is little variation in χ^2 value with such a change in β, the shape of our χ^2 contours for T_0 versus γ should be virtually independent of the actual value for β. From fits to the IPC data we have shown that the parameters β and γ are correlated (see Fig. 2) The values employed here came from the imaging analysis on the central field data only and ranged linearly from $\beta = 0.75$ (isothermal) to $\beta = 0.34$ (adiabatic).

The RS emission model was used to construct a grid of models with varying central temperature and polytropic index. Each of these models was compared to the *Tenma* data, minimizing χ^2 for the remaining parameters: overall normalization, elemental abundance (as above), and hydrogen column density. The results of these fits are presented in Figure 5*a* as two-dimensional χ^2 contours for γ versus T_0. We show the 90% and 99% confidence level contours. Clearly at the higher confidence level we are unable to put any constraint on the value of the polytropic index, although at 90% confidence we reject polytropic indices below ~ 1.1, indicating that the spectrum exhibits departures from isothermality. We note that the average temperature (weighted by the appropriate emission measure) can be quite accurately used to characterize the X-ray spectrum, since it varies only slightly from 7.5 ± 0.25 for the isothermal spectrum to 7.5 ± 0.6 for the adiabatic one.

e) Generalized Cavaliere and Fusco-Femiano Polytropic Models ($\alpha = 1/2$)

The result of fits to the *Tenma* spectrum for this model, corresponding to equation (4) with $\alpha = \frac{1}{2}$, is shown in Fig. 5*b*. As above the β values came from the IPC imaging analysis and varied from 1.68 (isothermal) to 0.86 (adiabatic). It is clear that we can reject polytropic indices greater than ~ 1.4 at the 90% confidence level, although at the 99% confidence level we must accept all indices. Recall that our purpose in introducing this generalized model was to obtain an acceptable fit to the X-ray imaging and spectral data for an adiabatic ($\gamma = 5/3$) model. This has been achieved at about the 99% confidence level. The best-fit parameter values for this adiabatic model are presented in the third column of Table 2. Notice that the elemental abundance is slightly larger than the isothermal value, a result of the presence of higher temperature emission components in the adiabatic case. Two-dimensional error contours (at 90% and 99%) for the fractional iron abundance versus central temperature are shown in Figure 4*b*. The central gas density from the normalization to the spectrum is $(3.6 \pm 0.2) \times 10^{-3}$ cm^{-3} using the fitted core radii from Table 1. This value is somewhat larger than (but still within the errors of) the central density determined from the normalization to the IPC surface brightness, perhaps signifying that there is more emission at the larger radii sampled by the *Tenma* instrument. Although this model seems to satisfy the combined X-ray imaging and spectral data, it becomes apparent upon closer examination that the implied total cluster mass is smaller than the gas mass required by the X-ray flux, a clear inconsistency. We discuss this in the following section.

IV. DISCUSSION

We use the results in Tables 1 and 2 along with equation (6) to determine the total cluster binding mass distribution implied by the isothermal and adiabatic models. For the best-fit isothermal model ($T_0 = 7.5$ keV, $\gamma = 1$, $r_c = 0.31$ Mpc, $\beta = 0.63$, $\alpha = 0$) the binding mass is $\sim 1.5 \times 10^{15}\ M_\odot$ within 3 Mpc and increases as r^1 to larger radii. The gas mass constitutes $\sim 8\%$ of the cluster binding mass at the center, increasing to $\sim 30\%$ at 10 Mpc. With the parameters for the best-fit adiabatic model ($T_0 = 20.5$ keV, $\gamma = 5/3$, $r_c = 0.22$ Mpc, $\beta = 0.86$, $\alpha = \frac{1}{2}$) the binding mass is $\sim 3.9 \times 10^{14}\ M_\odot$ within 1 Mpc and increases (asymptotically) to a maximum mass of only $\sim 4.2 \times 10^{14}\ M_\odot$. This is as expected from equation (6), since the mass varies as r^0 for $\alpha = \frac{1}{2}$ at large radii. However, when we compare the binding mass density with the gas density in this case, we find that near the center the implied total cluster binding mass density is 60 times the gas density, but beyond ~ 0.7 Mpc the binding mass density *falls below* the gas density, a clear physical impossibility. Although this adiabatic model adequately describes both the spectral and imaging X-ray data, it is internally inconsistent and so must be rejected. This evidence plus the internal inconsistency of the adiabatic model under the Henriksen and Mushotzky polytropic formulation (see eq. [8]), leads us to suggest that no adiabatic gas temperature distribution can describe the Coma cluster.

On the other hand, how well does an isothermal gas distribution fit the data? Comparison of Figures 2*a* and 5*a* reveals an apparent inconsistency between the imaging and spectral results for this model. While the imaging data require a nearly isothermal solution, the X-ray spectrum prefers nonisothermal temperature distributions. For models with $\alpha = \frac{1}{2}$ (Figs. 2*b* and 5*b*), the situation is reversed: the spatial data prefer nonisothermal distributions and the spectral data prefer nearly isothermal ones. Indeed, there are regions of overlap between the imaging and spectral results at intermediate values of γ in each case, but this cannot be considered to represent a definitive range on the acceptable temperature distribution. Our conclusion is that the X-ray data are now precise and detailed enough to require a more realistic model than a polytrope. Below we present a simple model which is fully consistent with both the imaging and spectral data and has the advantage of allowing

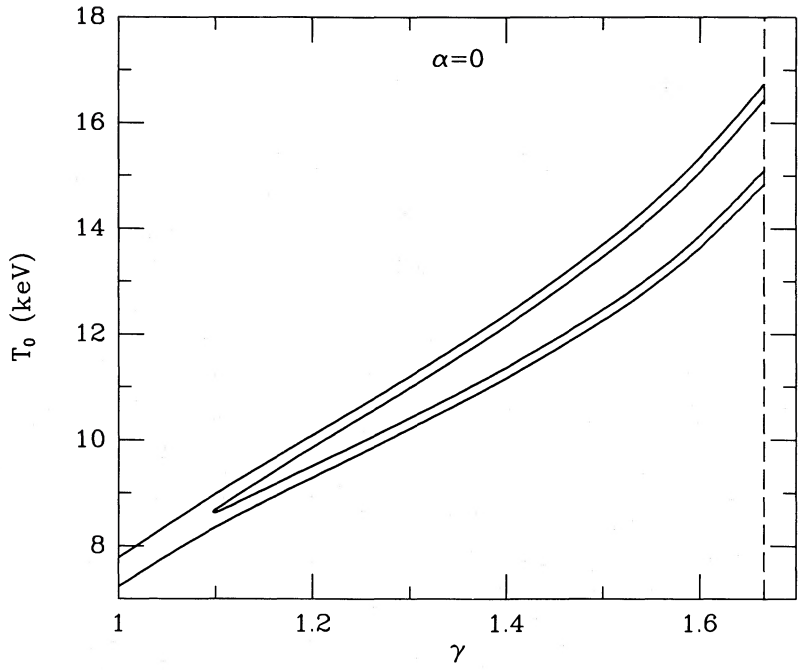

FIG. 5*a*

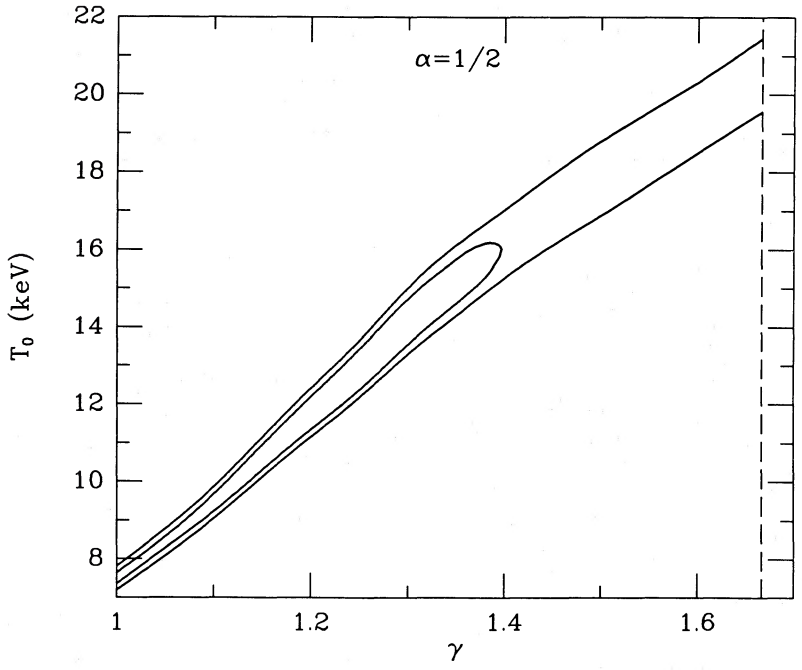

FIG. 5*b*

FIG. 5.—(*a*) Results of fits to the *Tenma* X-ray spectrum of Coma. Two-dimensional χ^2 contours (90% and 99% confidence levels) for polytropic index (γ) vs. central temperature (T_0) using the Cavaliere and Fusco-Femiano (1976, 1978) model ($\alpha = 0$). Indices range from $\gamma = 1$ (isothermal) to $\gamma = 5/3$ (adiabatic). (*b*) Same as (*a*) but for the $\alpha = \frac{1}{2}$ polytropic model.

us to quantify the extent of isothermality implied by the observations.

In introducing this hybrid model we have been strongly motivated by theoretical considerations of the effects of electron heat conduction on the cluster gas. In a cluster, conduction occurs most rapidly in the central region, where the densities and perhaps, temperatures are (initially) the highest, assuming an initial adiabatic infall of matter. In time, a conduction front moves out from the center, separating an approximately isothermal region within from the undisturbed medium beyond. If the conduction were inhibited by a small, but definitely nonzero, factor, then it would be possible for the front to have traveled only partly through the cluster in a Hubble time. This process could leave an isothermal core surrounded by a nonisothermal distribution. It is widely suspected that magnetic fields would inhibit conduction, but by how

much is an open question. Investigations such as this might be able to shed some light on the subject.

In addition we have been strongly guided by the X-ray data. For the standard Cavaliere and Fusco-Femiano polytropic models, as shown above, the spatial data require us to constrain the gas density to follow an isothermal distribution. However this constraint only applies over the central region (within ~ 4 core radii); beyond this radius there are presently no imaging data and hence no strong limits on the gas density profile. The spectral data come from a much larger spatial extent, $\sim 40\%$ of the emission in the *Tenma* field of view comes from beyond 4 core radii. Thus it seems reasonable to accommodate the spectral observations, which imply departures from isothermality, by situating the nonisothermal component outside the central region. This leads directly to our hybrid model, which is characterized by having an isothermal core surrounded by a polytropic distribution. Finally, we have opted for this model since it allows us to parameterize the departures from isothermality in a nearly model-independent way as a fraction of total cluster emission.

For the gas density, we have taken an isothermal radial profile with $\beta = 0.6$ (eq. [3]), assumed constant throughout the cluster. The temperature distribution is flat (i.e., isothermal) out to a certain transition radius, after which point it begins to fall off as a polytrope. Thus the isothermal region is defined by two parameters: its temperature and $R_{\rm ISO}$, the radius at which the temperature starts to vary. For the nonisothermal region we have used the polytropic formulation of Henriksen and Mushotzky (1985, 1986). However, as discussed above, in this model hydrostatic equilibrium is not guaranteed unless the condition given by equation (8) is satisfied. Thus the largest value for the index consistent with hydrostatic equilibrium, and our chosen density profile is $\gamma = 1.55$, which is the value we have used throughout the polytropic region. Note that this requirement is not an artifact of the *hybrid* model but corresponds to the steepest polytropic temperature profile consistent with hydrostatic equilibrium. A smaller value of γ would tend to increase the allowed isothermal region; hence our results here are in that sense a lower limit to the isothermal contribution.

In our fits to the *Tenma* data we have chosen to vary only the temperature of the isothermal region and $R_{\rm ISO}$. In principle, one could vary both γ and β in the region beyond where the imaging data ends, but we have left the parameters in the polytropic region fixed. For the particular parameterization discussed above we have obtained the two-dimensional χ^2 contours shown in Figure 6, where the allowed values of the isothermal temperature and transition radius are plotted. One sees that (at 90% confidence), based only on the spectral data, the radius of the isothermal region can be as small as ~ 1 core radius or as large as 6 core radii. In the top panel of Figure 6 we have also plotted the ratio of the emission measure of just the central isothermal region to the total emission in the *Tenma* field of view, $f_{\rm ISO}$. As much as $\sim 75\%$ of the observed emission in the *Tenma* spectrum can be coming from an isothermal component.

This model clearly establishes excellent consistency between the spatial and spectral data sets. Future work should include direct comparison of more detailed evolutionary models involving electron heat conduction, such as those presented in Friaca (1986), to the X-ray data. In addition the hybrid model in the form presented here predicts a break in the slope of the gas density profile at the transition radius, changing from isothermal to polytropic. Observing such a break in the X-ray

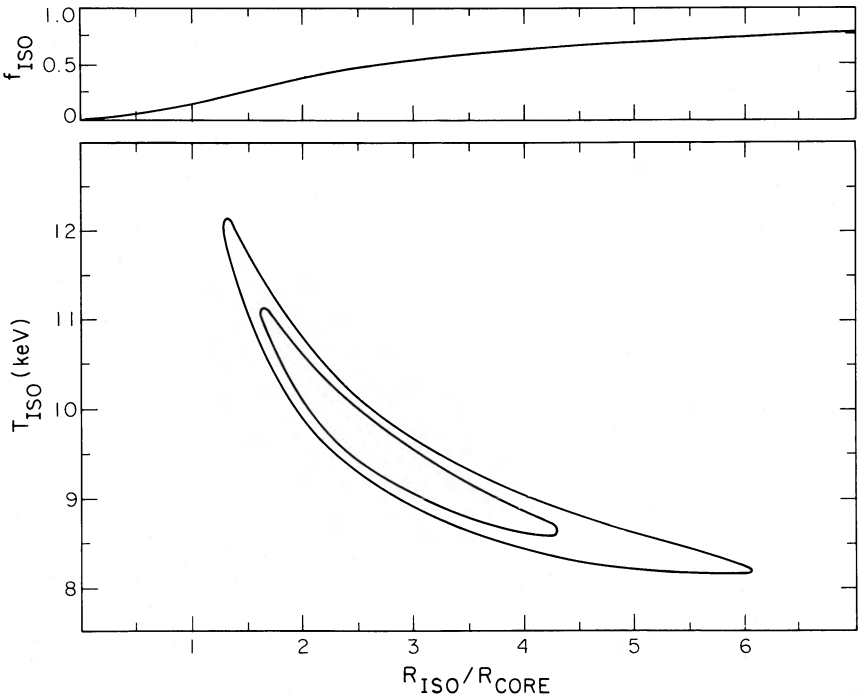

FIG. 6.—Results of fits to the *Tenma* spectrum of Coma for the hybrid model, consisting of an isothermal core surrounded by a polytropic distribution. *Bottom panel*: the two-dimensional χ^2 contours (68% and 90% confidence levels) for the temperature of the isothermal region ($T_{\rm ISO}$) versus its radius ($R_{\rm ISO}$) in units of the core radius. For the gas density $\beta = 0.6$ and for the polytropic region $\gamma = 1.55$. *Top panel*: the fraction of emission measure within the isothermal region relative to the total emission measure as a function of $R_{\rm ISO}$.

surface brightness profile would be strong evidence in support of the model.

VI. CONCLUSIONS

We have used the high-quality X-ray spectrum of the Coma cluster observed by the Japanese satellite *Tenma* in conjunction with the imaging data from the *Einstein Observatory* to explore the temperature distribution of the cluster gas. We have found that, although an adiabatic temperature distribution can satisfy the X-ray data, such a model is internally inconsistent, either implying more gas mass than total binding mass, or requiring nonhydrostatic conditions in the cluster gas. Even the best-fit isothermal model ($T_0 = 7.5$ keV, $\gamma = 1$, $r_c = 0.31$ Mpc, $\beta = 0.63$, $\alpha = 0$) does not fully satisfy the *Tenma* spectrum; we find evidence at the 90% confidence level for a nonisothermal distribution of temperatures. The iron abundance we determine from the spectrum depends only slightly on model and is significantly less than the cosmic value (16.2%–32.5% at 99% confidence). This is the most precise determination yet of the iron abundance in this (or any) cluster. Note that the experimental errors on the derived iron abundance are now comparable to the errors from theoretical uncertainties in the atomic physics. For the isothermal model the total mass of the Coma cluster is $\sim 1.5 \times 10^{15} M_\odot$ within 3 Mpc ($H = 50$ km s^{-1} Mpc^{-1}), and beyond this it increases linearly with radius. We have shown that it is possible to obtain much smaller values for the binding mass from the X-ray data alone. These values in some cases are smaller than the mass of gas required by the X-ray luminosity of the cluster (as in our adiabatic model) and can be rejected on that basis. Further progress on determining the mass of the cluster will come from a combined analysis of the X-ray and optical data (Hughes 1988).

The main conclusion of the combined spatial and spectral analysis of the Coma cluster presented in this paper is that pure polytropic models are inadequate to describe the temperature distribution of the cluster gas. The X-ray data have advanced to the stage now that the use of polytropic models leads to inconsistencies between the spectrum and the spatial data. This should come as no surprise since, as Perrenod (1978) and more recently Friaca (1986) have pointed out, realistic models for the evolution of the cluster gas *do not* look like polytropes. The task now is to construct simple parameterizations which can be used as a bridge between the data and more realistic models. As a first attempt at this, we have introduced a simple model for the temperature distribution which consists of an isothermal core region surrounded by a polytropic distribution. This approach has been able to describe the imaging and spatial data in a consistent manner and strongly implies that the center of the Coma cluster can have an isothermal distribution out to as much as 6 core radii. Indeed up to 75% of the cluster X-ray emission can be coming from an isothermal component. This result should have a significant impact on future models for the evolution of the cluster gas, in particular regarding the role of thermal conduction.

One of the authors (J. P. H) would like to extend his thanks to Y. Tanaka and the group at ISAS for their kind hospitality and financial support during his stay in Japan. We would like also to acknowledge useful discussions with K. Arnaud, D. Fabricant, W. Forman, J. Grindlay, C. Jones, and W. Tucker.

REFERENCES

Abramopoulos, F., Chanan, G. A., and Ku, W. H.-M. 1981, *Ap. J.*, **248**, 429.
Avni, Y. 1976, *Ap. J.*, **210**, 642.
Bahcall, J. N., and Sarazin, C. L. 1978, *Ap. J.*, **219**, 781.
Bertschinger, E., and Meiksin, A. 1986, *Ap. J. (Letters)*, **306**, L1.
Cavaliere, A., and Fusco-Femiano, R. 1976, *Astr. Ap.*, **49**, 137.
———. 1978, *Astr. Ap.*, **70**, 677.
Cowie, L. L., Henriksen, M., and Mushotzky, R. 1987, *Ap. J.*, **317**, 593.
Friaca, A. C. S. 1986, *Astr. Ap.*, **164**, 6.
Giacconi, R., *et al.* 1979, *Ap. J.*, **230**, 540.
Gorenstein, P., Fabricant, D., Topka, K., and Harnden, F. R., Jr. 1979, *Ap. J.*, **230**, 26.
Henriksen, M. J., and Mushotzky, R. F. 1985, *Space Sci. Rev.*, **40**, 681.
———. 1986, *Ap. J.*, **302**, 287.
Hughes, J. P. 1988, in preparation.
Kellogg, E., Baldwin, J. R., and Koch, D. 1975, *Ap. J.*, **199**, 299.
King, I. 1972, *Ap. J. (Letters)*, **174**, L123.
Koyama, K., *et al.* 1984, *Pub. Astr. Soc. Japan*, **36**, 659.
Lampton, M., Margon, B., and Bowyer, S. 1976, *Ap. J.*, **208**, 177.
Lea, S. M. 1975, *Ap. Letters*, **16**, 141.
Matteson, J. L. 1971, Ph. D. thesis, University of California, San Diego.
Maxon, M. S., and Corman, E. G. 1967, *Phys. Rev.*, **163**, 156.
Mitchell, R. J., Culhane, J. L., Davison, P. J. N., and Ives, J. C. 1976, *M.N.R.A.S.*, **176**, 29.
Mushotzky, R. F., Serlemitsos, P. J., Smith, B. W., Boldt, E. A., and Holt, S. S. 1978, *Ap. J.*, **225**, 21.
Okumura, Y., Tsunemi, H., Yamashita, K., Matsuoka, M., Koyama, K., Hayakawa, S., Masai, K., and Hughes, J. P. 1988, *Pub. Astr. Soc. Japan*, submitted.
Perrenod, S. C. 1978, *Ap. J.*, **226**, 566.
Raymond, J. C., and Smith, B. W. 1977, *Ap. J. Suppl.*, **35**, 419 (RS).
Rosner, R., Tucker, W. H., and Najita, J. 1988, *Ap. J.*, submitted.
Sarazin, C. L. 1986, *Rev. Mod. Phy.*, **58**, 1.
Sarazin, C. L., Rood, H. J., and Struble, M. F. 1982, *Astr. Ap.*, **108**, L7.
Serlemitsos, P. J., Smith, B. W., Boldt, E. A., Holt, S. S., and Swank, J. H. 1977, *Ap. J. (Letters)*, **211**, L63.
Tanaka, Y., *et al.* 1984, *Pub. Astr. Soc. Japan*, **36**, 641.

JOHN P. HUGHES: Harvard-Smithsonian Center for Astrophysics, 60 Garden Street, Cambridge, MA 02138

MASARU MATSUOKA: Cosmic-Ray Laboratory, The Institute of Physical and Chemical Research, 2–1 Hirosawa, Wako, Saitama 351, Japan

YOSHIHARU OKUMURA: Toray Industries, Inc., Otsy, Shiga 520, Japan

HIROSHI TSUNEMI, and KOUJUN YAMASHITA: Department of Physics, Faculty of Science, Osaka University, Toyonaka, Osaka 560, Japan